Cancer & Metabolism

RESEARCH Open Access

PAF1/HIF1α axis rewires the glycolytic metabolism to fuel aggressiveness of pancreatic cancer

Ayoola O. Ogunleye[1], Neelanjana Gayen[1], Sanchita Rauth[1], Saravanakumar Marimuthu[1], Rama Krishna Nimmakayala[1], Zahraa W. Alsafwani[1], Jesse L. Cox[2], Surinder K. Batra[1,3*] and Moorthy P. Ponnusamy[1,3*]

Abstract

Background PAF1/PD2 deregulation contributes to tumorigenesis, drug resistance, and cancer stem cell maintenance in Pancreatic Cancer (PC). Recent studies demonstrate that metabolic reprogramming plays a role in PC progression, but the mechanism is poorly understood. Here, we focused on examining the role of PAF1/PD2 in the metabolic rewiring of PC.

Methods Cell lines were transfected with shRNAs to knockdown PAF1/PD2. Metabolic genes regulated by PAF1/PD2 were identified by qPCR/western blot, and metabolic assays were performed. Immunoprecipitations/ChIP were performed to identify PAF1/PD2 protein partners and confirm PAF1/HIF1α sub-complex binding to LDHA.

Results PAF1 and LDHA showed progressively increased expression in human pancreatic tumor sections. Aerobic glycolysis genes were downregulated in PAF1-depleted PC cells. Metabolic assays indicated a decreased lactate production and glucose uptake in knockdown cells. Furthermore, PAF1/PD2 depletion showed a reduced glycolytic rate and increased oxidative phosphorylation by ECAR and OCR analysis. Interestingly, we identified that HIF1α interacts and co-localizes with PAF1, specifically in PC cells. We also observed that the PAF1/PD2-HIF1α complex binds to the LDHA promoter to regulate its expression, reprogramming the metabolism to utilize the aerobic glycolysis pathway preferentially.

Conclusion Overall, the results indicate that PAF1/PD2 rewires PC metabolism by interacting with HIF1α to regulate the expression of LDHA.

Keywords Pancreatic cancer, Metabolism, Aerobic glycolysis

*Correspondence:
Surinder K. Batra
sbatra@unmc.edu
Moorthy P. Ponnusamy
mpalanim@unmc.edu
[1]Department of Biochemistry and Molecular Biology, Eppley Institute for Research in Cancer and Allied Diseases, University of Nebraska Medical Center, Nebraska Medical Center, Omaha, NE 985870, USA
[2]Department of Pathology and Microbiology, University of Nebraska Medical Center at Omaha, Omaha, NE, USA
[3]Fred and Pamela Buffett Cancer Center, Eppley Institute for Research in Cancer and Allied Diseases, University of Nebraska Medical Center at Omaha, Omaha, NE, USA

Introduction

Pancreatic Ductal Adenocarcinoma (PDAC), the most common type of pancreatic cancer (PC), is an aggressive disease with a 5-year survival rate of approximately 12.5%. It is currently the third leading cause of cancer-related deaths in the United States, with an estimated 64,050 cases and 50,550 deaths in 2023 [1]. Emerging studies indicate that metabolomic rewiring is involved in the progression and aggressiveness of several cancers, including PC. For instance, Karasinska et al. showed that PCs with transcriptional glycolysis, KRAS, and MYC gene amplification have a poor prognosis in resectable and metastatic cases [2]. Another study on quasi-mesenchymal (QM) PDAC, which are generally very aggressive and chemoresistant with FOLFIRINOX, reveals their dependency on glycolysis. Furthermore, the study showed that these QM cells produce and utilize lactate for its growth and survival [3]. Similarly, another study revealed that PDAC exhibited increased lactate production through aerobic glycolysis due to the upregulation of LDHA, therefore promoting pancreatic cancer cell growth [4]. Alternatively, PDAC cells with KRAS mutation could also be addicted to an alternative metabolic route involving glutamine (Gln) metabolism by regulating the expression of major metabolic enzymes such as glutamate dehydrogenase 1 (GLUD1) and aspartate transaminase (GOT1), which supports the rapid proliferation of cancer cells and maintaining redox balance in PDAC cells [5].

RNA Polymerase II-Associated Factor 1 (PAF1)/Pancreatic Differentiation 2 (PD2) is a transcription elongation factor and a member of the PAF1 complex (PAF1C) subunits, comprising other subunits (LEO1, CTR9, CDC73, SKI8). Previous studies from our lab demonstrated that deregulation of PAF1 is essential for the proliferation, progression, metastasis, and invasion of PC, and its loss promotes acinar-to-ductal metaplasia during PC initiation [6–9]. In addition, other studies have shown that PAF1 plays a critical role in the maintenance of cancer stem cells [10, 11]. Furthermore, several studies in acute myeloid leukemia, cervical, and lung cancers have also provided evidence that PAF1 is essential in developing and progressing these cancers [12–14]. Besides, emerging studies indicate that metabolic rewiring plays a significant role in pancreatic cancer progression [15]; however, the oncogenic master regulator of cancer metabolism is poorly understood. While most of these studies have provided evidence of the multifunctional nature of PAF1 in many kinds of cancers and elucidated its involvement in most of the hallmarks of cancer, there has been no study investigating the involvement of PAF1 during the metabolic alteration of cancer.

Hypoxia-inducible factor-1 alpha (HIF-1α) is a crucial transcription factor in cancer progression and metabolism, which acts differently depending on the presence or absence of oxygen [16]. It also regulates the transcription of numerous genes of glycolytic enzymes and glucose transporters [17]. The hypoxic nature of the tumor microenvironment of PC, resulting from the rapid proliferation of cells, poor vascularization, and desmoplastic regions, leads to an increase in the expression of HIF1α, which has been consistently implicated in the regulation of glycolytic genes [17–19]. Despite numerous studies affirming the multifunctional role of PAF1 in different facets of cancer, the role of PAF1 in the HIF1α-mediated metabolic reprogramming of PC is unknown. This study demonstrated that PAF1 is required for the metabolic alteration of PC.

Methods

Cell culture and treatments

Human PC cell lines SW1990, MIA PaCa-2, HPNE, and HPDE, were obtained from American-type culture collection (Manassas, VA, USA). SW1990 and MIA PaCa-2 cells were cultured in DMEM media (HyClone Laboratories, Logan, UT, USA), which was supplemented with 10% fetal bovine serum (FBS) (Sigma-Aldrich, St Louis, MO, USA) and 1% penicillin-streptomycin solution (Sigma). HPDE was cultured in human keratinocyte serum-free media supplemented with epidermal growth factor 1–53 (EGF 1–53) and bovine pituitary extract (BPE) (Gibco). HPNE was cultured in Dulbecco's modified Eagle's medium (low glucose) with 25% M3 Base Media (Incell, San Antonio, TX), supplemented with 5% (vol/vol) fetal bovine serum (FBS), 10 ng/mL epidermal EGF, and antibiotics (100 units/mL penicillin and 100 µg/mL streptomycin). Cells were incubated in a humidified incubator at 37 °C and supplied with 5% CO_2. For hypoxic treatment, cells were maintained in a humidified environment at 37 °C, 1% O_2 and 5% CO_2 tissue-culture incubator. Cells were sub-cultured by trypsin-EDTA treatment.

Depletion of PAF1 using shRNA

PAF1 knockdown in SW1990 and MIA PaCa-2 cells was performed using lentiviral human PAF1 shRNAs from Origene (Cat#RC200103L4V). HEK293T cells were cultured and transduced with Scr and shPAF1 plasmids to generate viral supernatant according to the manufacturer's instructions. A virus supernatant was used to infect SW1990 and MIA PaCa-2 cells. 72 h after transfection, GFP-positive cells were isolated by flow cytometry, and the GFP-positive population was collected in a 6-well plate, after which the cells were selected using puromycin (6 µg/ml for SW1990 and 2 µg/ml for MIA PaCa-2). shRNA-mediated knockdown of PAF1 expression was analyzed by immunoblot assay.

Quantitative PCR

Total RNA was isolated using the RNeasy mini kit (Qiagen 74106). Reverse transcription was performed from 1 μg of total RNA utilizing an iScript cDNA synthesis kit (BioRad 1708890). Quantitative PCR was performed using SYBR Green dye (Roche 04887352001) and a CFX Connect Real-Time PCR detection system (BioRad 1855200). Reactions were performed in triplicate, and β-actin was used as a control. The following primer pairs were used:

PAF1 forward 5′-TCTGTGAAGCAGCAGTTTACC −3′ and PAF1 reverse 5′-GAGATTGATTTCTGGG CATCCT −3′;
GLUT1 forward 5′- GATTGGCTCCTTCTCTGTG G −3′ and GLUT1 reverse 5′- TCAAAGGACTTGC CCAGTTT −3′;
ENO1 forward 5′- CTGGTGCCGTTGAGAAGGG −3′ and ENO1 reverse 5′- GGTTGTGGTAAACCT CTGCTC −3′;
PDK1 forward 5′- GTGGTTTATGTACCATCCCAT CTCT −3′ and PDK1 reverse 5′- TCCATAGTGGCT CTCATTGCAT −3′.
HK2 forward 5′- GAAGGTGGAGATGGAGAATCA G −3′ and HK2 reverse 5′- CCAGGAAACTCTCGT CTAGTTTAG −3′;
PKLR forward 5′- TCCCACACACAAACCAAGAG −3′ and PKLR reverse 5′- CCCTCTCCTACTCTAC AGCATTA −3′,
HK1 forward 5′- GTCACGATGTAGCCACTTTAC −3′ and HK1 reverse 5′-CGATGAGTCCAATCTCA CAAG −3′,
LDHA forward 5′- GCCTGTATGGAGTGGAATGA A −3′ and LDHA reverse 5′-CCAATAGCCCAGGA TGTGTAG −3′.

Western blotting assay

Cells were lysed in RIPA buffer (50 mM Tris-HCl, 150 mM NaCl, 1% NP-40, 0.5% sodium deoxycholate, 0.1% sodium dodecyl sulfate [SDS]) containing protease inhibitors (1 mM phenyl-methyl sulphonyl fluoride, 1 μg/ml aprotinin, 1 μg/ml leupeptin). Cell lysates were spun at 13,000 rpm for 30 min to remove debris, and protein quantification was performed using the Bio-Rad DC Protein Assay kit (RRID: SCR_008426). Total protein (45 μg/well) was fractionated by 10% SDS–PAGE. Fractionated proteins were transferred to polyvinylidene difluoride (PVDF) membranes. Membranes were blocked in 5% non-fat dry milk in PBS containing 0.1% Tween 20 (PBST). Blots were incubated overnight at 4 °C with primary antibodies: LDHA (1:1000, santacruz Cat# sc-137243), PDK1 (1:1000, Invitrogen Cat# MA5-15797), Glut1(1:2000, Invitrogen Cat# MA5-43799), PAF1 (1:5000, Bethyl Laboratories Cat#A300-173 A), and PDHA1 (1:1000, Invitrogen Cat#459400), and β-actin (1:5000 Sigma-Aldrich Cat#A1978-200ul). β-actin was used as a loading control for protein normalization. The membranes were then washed in PBST, probed with the appropriate secondary antibodies, incubated for an hour at room temperature, and then washed with PBST. Signals were detected with the Pierce ECL Western Blotting Substrate kit (Thermo Scientific).

Immunoprecipitation assay

Immunoprecipitation assay was performed using Dynabeads Protein G immunoprecipitation kit (Invitrogen Cat#10007D). Cells were lysed in IP lysis buffer (Thermo Scientific Cat#87787) mixed with Halt protease and phosphatase inhibitor cocktail (Invitrogen Cat#78440). Protein lysates (500 μg) were immunoprecipitated with 2 μg of rabbit anti-PAF1 antibody (Abcam Cat#ab20662) or mouse anti-HIF1α antibody (BD Biosciences Cat# 610959). First, 20 μl of dynabeads were incubated with rabbit anti-PAF1 antibody or rabbit anti-HIF1α antibody in 'antibody binding and washing buffer' on a shaker for 1 h at room temperature. After washing, the antibody-bound beads were incubated with protein lysates overnight at 4 °C. The next day, the immune complex on beads was washed three times with washing buffer, and the sample was eluted in the elution buffer. The eluted samples were mixed with 5x Lane Marker Non-Reducing Sample Buffer (Thermo Scientific Cat#39001) and heated at 950 C for 5 min before loading in 10% SDS-PAGE gel. The immunoprecipitated products were subjected to 10% SDS-PAGE, then transferred onto a PVDF membrane and immunoblotted with mouse anti-HIF1α antibody 1:250 (BD Biosciences Cat# 610959) or rabbit anti-PAF1 antibody 1:5000 (Bethyl Laboratories Cat#A300-172 A). After washing, the membranes were incubated with Goat anti-rabbit or anti-mouse IgG secondary antibody or HRP (Invitrogen Cat#31460) or Clean-Blot IP detection kit (HRP) (Invitrogen Cat#21232).

Chromatin immunoprecipitation (ChiP) assay

ChiP assay was performed by seeding cells and fixing the cells with 0.4% formaldehyde and 1.5 mM EGS (ethylene glycol bis (succinimidyl succinate) (Thermo Scientific Cat#21565), washed, collected, and resuspended in 500 μl SDS lysis buffer (1% SDS, 10 mM EDTA, 50 mM Tris-HCl [pH 8.1], 1 mM PMSF, and 1 μg/ml aprotinin). Then, the samples were sonicated and diluted in ChIP dilution buffer (0.01% SDS, 1.1% Triton X-100, 1.2 mM EDTA, 16.7 mM Tris-HCl [pH 8.1], 167 mM NaCl, 1 mM PMSF, and 1 μg/ml aprotinin). 10% of sonicated samples were separated for the input control. Chromatin was immunoprecipitated with rabbit anti-PAF1 antibody (Abcam Cat#ab20662). Chromatin extracts were pulled down

with Dynabeads Protein G. The samples were washed extensively with wash buffers (low salt, high salt, LiCl, and Tris/EDTA buffers), eluted with SDS elution buffer, and subjected to reverse cross-linking and proteinase digestion. As a control, IgG antibody was used for the ChIP assay. The captured and purified DNA was subjected to PCR amplification using the LDHA gene promoter primers spanning three HIF1α binding sites (B.S.), using the following primers: HIF1α B.S.1 forward 5′- C TGACTGACTGCTAGGCATTT-3' and HIF1α B.S.1 reverse: 5'- GGAAGGCTTGGATCTGTTTCT −3'. HIF1 B.S.2/3 forward 5′- GTGCCTATTACGTGCCAGAA-3' and PAF1 B.S.2/3 reverse: 5'- GACGACCTTCAGTTTC CTCATC −3'.

Immunohistochemistry

Tissue microarray (TMA), CP (US Biomax Cat# BIC14011b) was purchased, and the tissue samples from the normal pancreas ($n=6$), chronic pancreatitis (CP) ($n=16$), PanIN1 ($n=8$), PanIN2 ($n=3$), PanIN3 ($n=6$), and PDAC ($n=8$) are included in the TMA. The TMA was subjected to immunohistochemical staining by using the following primary antibodies at the indicated dilution: PAF1 1:100 (Bethyl Laboratories Cat#A300-173 A) and LDHA 1:100 (Santacruz Cat# sc-137243). Antigen retrieval was performed in 10 mM sodium citrate buffer (pH 6). The stained sections were scored blindly. The intensity of protein expression was graded on a scale of 0 to 3 (0, no staining; 1+, weakly positive; 2+, moderately positive; 3+, strongly positive). The percentage of positive staining was scored in the range of (0–100% or 0–1). A histoscore was calculated by multiplying intensity (0–3) and positivity (0–1), ranging between 0 and 3. GraphPad Prism software (RRID: SCR_002798) was used to calculate *P* values.

Immunofluorescence analysis

For cells, the cells were plated onto sterile round coverslips (CIR 18−1 Fisher brand 12-545-10, Fisher Scientific International, Hampton, NH, USA) and grown in 12-well plates. After 24 h, cells were fixed in 100% methanol (pre-chilled in −20 °C). The cells were washed in PBS and blocked with 10% normal goat serum (NGS) for 2 h. For tissues, harvested tissues were fixed in 10% formalin and embedded in paraffin. Briefly, slides were baked for 2 h at 60 °C, deparaffinized in xylene, and rehydrated sequentially in ethanol. For antigen retrieval, slides were microwaved in sodium citrate buffer for 15 min. Slides were blocked in 5% normal goat serum. The cells/tissue sections were incubated with primary antibody rabbit-PD2 (1: 300), rabbit-HIF1α (1: 300), and mouse-LDHA (1: 300) overnight. The next day, the cells and tissue sections were washed with PBST four times (10 min each) and incubated with fluorescent-tagged secondary antibodies—both FITC and Texas-red tagged (for 30 min) at room temperature and washed four times with PBST. Finally, coverslips were mounted with a vectashield mounting medium containing DAPI (VECTOR, Burlingame, CA, USA). Confocal images were collected using a Zeiss LSM800 confocal microscope with a 63×/1.4 NA oil objective. The images were quantified by measuring the mean fluorescent intensity of the cells and tissues of each group. Data was normalized with the intensity of DAPI in each image.

Glucose uptake and lactate release assay

Ten thousand cells were seeded per well (six replicates per cell type) in 96-well white transparent flat bottom tissue culture plates (Corning, ME, USA). Glucose uptake and lactate release assays were performed using the Glucose Uptake-Glo™ Assay kit (Promega Cat# J1341) and Lactate-Glo™ Assay kit (Promega Cat# J5021) by following the manufacturer's protocol. Luminescence readings were taken using a Synergy Neo2 multimode reader (BioTek, VT, USA).

Extracellular acidification rate (ECAR) measurement

Twenty thousand cells were plated in XF96 cell culture microplates (Seahorse Biosciences, Cat# 101085-004). After 24 h, the growth medium was replaced with XF assay medium (Seahorse Biosciences, Cat# 103334-100), followed by incubation at 37 °C for one hour in a CO2-free incubator. The basal ECAR and the ECAR following the addition of glucose (10 mM), oligomycin (1 μM), and 2-deoxyglucose (50 mM) were measured using an XF96 extracellular flux analyzer (Seahorse Biosciences) by following the manufacturer's protocol. The ECAR values were normalized to total cell counts in each well.

Oxygen consumption rate (OCR) measurement

Twenty thousand cells were plated in XF96 cell culture microplates (Seahorse Biosciences, Cat# 101085-004). After 24 h, the growth medium was replaced with XF assay medium (Seahorse Biosciences, Cat# 103334-100), followed by incubation at 37 °C for 1 h in a CO2-free incubator. The basal OCR and the OCR following the addition of oligomycin (1 μM), FCCP (0.5 μM), and rotenone/antimycin A (0.5 μM) were measured using XF96 extracellular flux analyzer (Seahorse Biosciences) by following the manufacturer's protocol. The OCR values were normalized to total cell counts in each well.

Results

PAF1 expression correlates with aerobic glycolysis pathway genes in PDAC

To examine the correlation between PAF1 and metabolic pathways, we performed a correlation analysis using PAF1 as the selected gene for the PC sample type

and customized the corGSEA to hallmark. The analysis revealed that PAF1 expression in PC is enriched and statistically significant in various metabolic pathways, including oxidative phosphorylation and glycolysis (Fig. 1A and B). Next, we investigated the correlation between PAF1 expression and individual genes of aerobic glycolysis and oxidative phosphorylation pathways. Upon further investigation, we observed that PAF1 correlated positively with the primary genes of the aerobic glycolysis pathway (Fig. 1C). To explore further the relationship

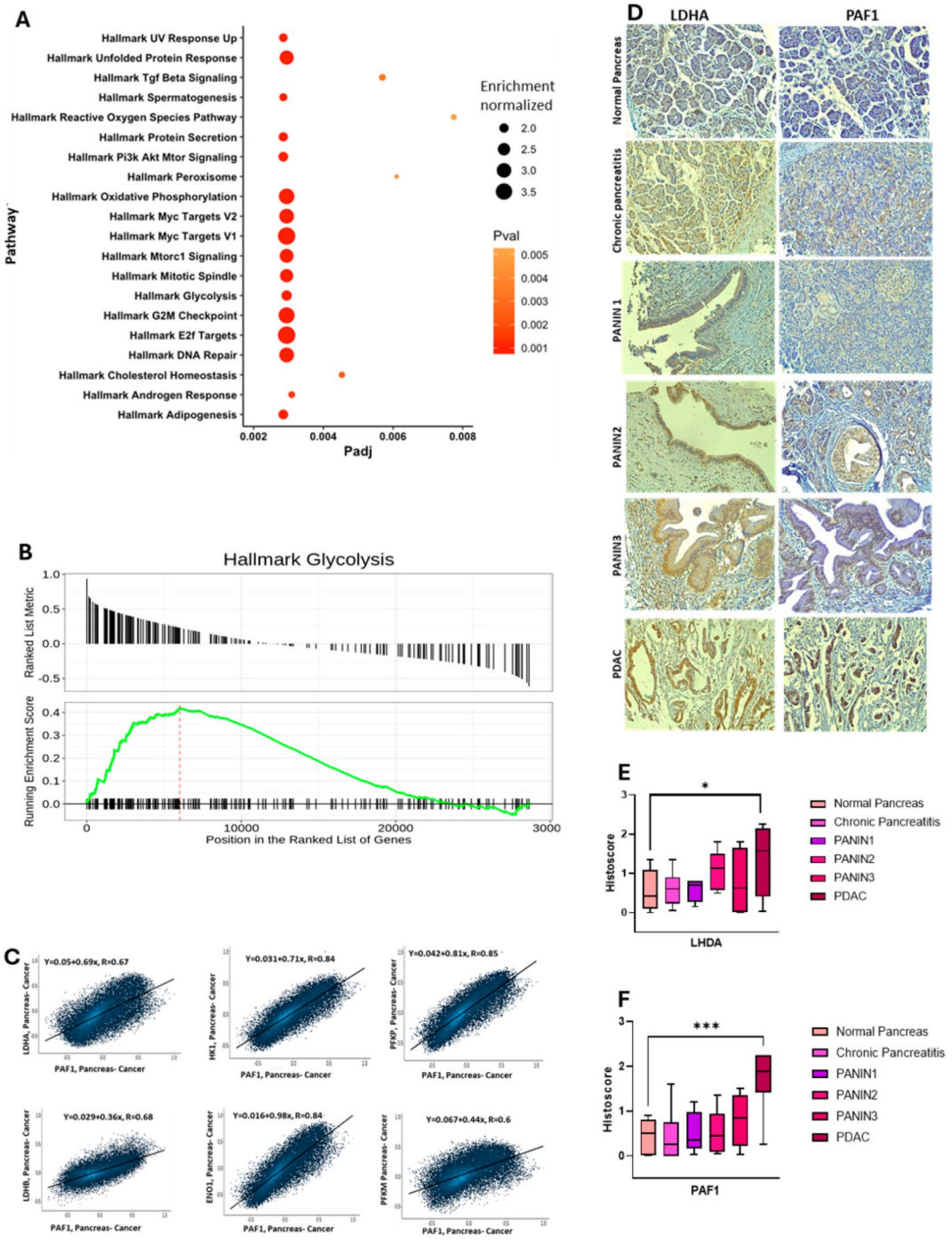

Fig. 1 PAF1 correlates with the aerobic glycolysis pathway genes in PDAC. **A** Single gene analysis of PAF1 with multiple pathways. **B** Enrichment plot of glycolysis pathway in pancreatic cancer. **C** Correlation analysis between PAF1 and genes of the aerobic pathway **D.** Immunohistochemical analysis of PAF1 and LDHA in PDAC progression tissue samples. **E**, **F**. A histoscore was calculated by multiplying intensity and positivity. Images were captured at ×20 magnification. Data represents mean ± SD. P-values were calculated using ordinary one-way ANOVA (multiple comparisons). $*p < 0.05$, $***p<0.001$

between PAF1 expression and aerobic glycolysis pathway, the expression of PAF1 and LDHA (the rate-limiting key factor of the pathway) were quantified by performing immunohistochemical staining. The staining revealed a basal/low expression of both PAF1 and LDHA in the normal pancreas (Fig. 1D). However, PAF1 and LDHA expression was gradually elevated in chronic pancreatitis and PanINs, with both expression significantly highest (p=0.0005-PAF1; p=0.0396-LDHA) in PDAC, as evidenced in the histoscore (Fig. 1E, F). These observations suggest a probable link between PAF1 and LDHA during the development and progression of PDAC.

PAF1 depletion decreases the expression of aerobic glycolytic genes in PC

Since LDHA was the rate-limiting step in aerobic glycolysis, we carried out immunofluorescence staining to examine the co-expression between LDHA and PAF1 using human PDAC (MIA PaCa-2 and SW1990) cell lines. We observed a high expression of PAF1 and LDHA, as well as a co-expression, in human PC cell lines, MIA-PaCa-2 and SW1990, compared to HPDE, where there was little expression of both PAF1 (p=0.0021; p=0.0130) and LDHA (p=0.0051; p=0.0323) (Fig. 2A and B). Furthermore, this was validated in human PC tissues. While there was high expression of both PAF1 (p=0.0057) and LDHA (p=0.0136) in human PC tissues, a low and basal expression of both proteins was observed in normal pancreas (Fig. 2C and D). These results suggest that the co-expression between LDHA and PAF1 may contribute to the progression of PDAC.

Next, we investigated the effect of PAF1 expression on aerobic glycolysis genes. Using shRNA, we developed PAF1 knockdown PC cells (MIA PaCa-2 and SW1990) and analyzed the critical regulators of the aerobic glycolysis pathway. Interestingly, results showed that PAF1 knockdown in MIA PaCa-2 and SW1990 cells decreased the expression of aerobic glycolysis genes including LDHA, PDK1 and GLUT1 in both mRNA levels (Fig. 2E, F) and protein levels (Fig. 2G). This observation was consistent in both MIA PaCa-2 and SW1900 except PDHA1, whose mRNA and protein levels increased significantly upon PAF1 depletion. Furthermore, we observed that PAF1 knockdown cells had a significantly reduced clonogenic growth based on the number of colonies formed, compared to Scr (Supplementary Fig. 2A). These results suggest that PAF1 plays a role in the expression of aerobic glycolysis genes.

PAF1 depletion decreases lactate production and glucose uptake in PDAC

To further investigate the role of PAF1 overexpression in the aerobic glycolysis pathway, we measured the extracellular lactate concentration by performing lactate assay in shPAF1 MIA PaCa-2 and SW1990 cells, thereby assessing the LDH enzymatic activity in the presence and absence of PAF1. The lactate assay showed a significant decrease (p=<0.0001- MIA PaCa-2; p = <0.0001-SW1990) in the extracellular lactate released in PAF1 knockdown cells (Fig. 3A) compared to the control (Scr) cells, suggesting a compromised LDH activity in the PAF1-depleted cells. A similar trend was observed in the glucose uptake assay performed, as PAF1 knockdown cells had significantly (p=<0.0001- MIA PaCa-2; p- <0.0001-SW1990) lower glucose uptake levels compared to their control/Scr counterpart (Fig. 3B), suggesting an association between PAF1 overexpression and the ability of PC cells to absorb glucose and metabolize it than normal cells.

PAF1 deletion suppresses glycolysis and increases mitochondrial respiration in PDAC cells

To explore the effect of PAF1 knockdown on the cellular bioenergetics of PC cell lines, the extracellular acidification rate (ECAR) of MIA PaCa-2 and SW1990 Scr and PAF1-depleted cells were analyzed using the extracellular flux analyzer. PAF1 knockdown cells had significantly decreased aerobic glycolytic rate in MIA PaCa-2 and SW1990 (Fig. 3C) compared to Scr cells. Furthermore, various parameters of the aerobic glycolytic rate were analyzed. The results showed that PAF1 knockdown decreased maximal glycolytic rate and glycolytic capacity in MIA PaCa-2 and SW1990 cells. In addition, PAF1 knockdown reduced basal and maximum levels of glycolysis, inhibiting glucose metabolism in MIA PaCa-2 and SW1990 cells. These data suggested that PAF1 knockdown suppressed glycolysis in PDAC cells.

To further investigate the effects of PAF1 knockdown on PDAC bioenergetics, we assessed oxidative phosphorylation by measuring cellular oxygen consumption rate (OCR) in MIA PaCa-2 and SW1990 Scr and PAF1-depleted cells. OCR was significantly increased in PAF1 knockdown cells compared to Scr cells (Fig. 3D). Additionally, the indices of mitochondrial respiration were assessed. The data indicated that PAF1 knockdown dramatically increased maximal respiration in MIA PaCa-2 and SW1990 cells. Furthermore, ATP-linked respiration and basal respiration were also affected, as these indices were increased. Overall, the data indicated that PAF1 knockdown led to an increase in mitochondrial respiration.

PAF1 interacts with HIF1α specifically and independently in PC

Next, we investigated the mechanism through which PAF1 could alter metabolism in PDAC. We analyzed the GEPIA2 portal to investigate the correlation between PAF1 and essential transcription factors commonly implicated in aerobic glycolysis. Interestingly, of all the

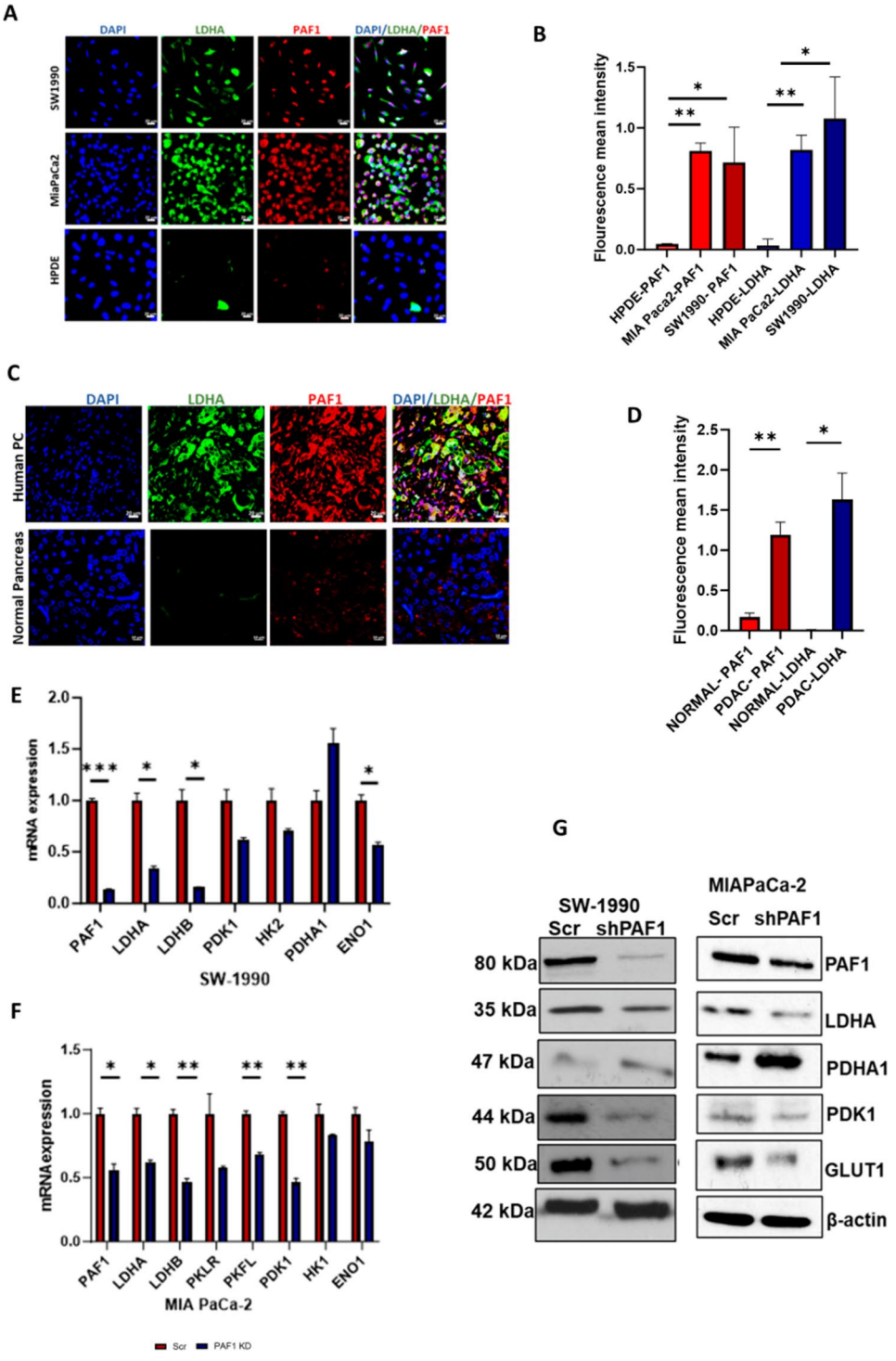

Fig. 2 Co-expression of PAF1/LDHA in PC models and loss of PAF1 reduces aerobic glycolytic genes expression. **A.** Immunofluorescence images of SW1990, MIA PaCa-2 and HPDE cell lines stained with PAF1 and LDHA antibody. Scale bar 20 µm **B**. Fluorescence mean intensity quantification of LDHA and PAF1 expression in Fig. 2 (**A**) **C**. Immunofluorescence images of Human PDAC and normal pancreas tissues stained with PAF1 and LDHA antibody. Scale bar 20 µm. **D**. Fluorescence mean intensity quantification of LDHA and PAF1 expression in Fig. 2 (**C**). Quantitative real-time PCR (qRT-PCR) analysis of PAF1, LDHA, LHHB, PDK1, HK2, PDHA1, ENO1, PKFL, PKFR, HK1 in Scr and PAF1 KD **(E)** SW1990 and **(F)** MIA PaCa-2 cells, qRT-PCR data were normalized with the β-Actin gene. **(G)** Western blot analysis of PAF1 and aerobic glycolysis genes expression in PAF1 KD and scramble SW1990 and MiaPaCa2 cells. β-actin was used as a control. Data are presented as the mean ± SD (*p<0.05,**p<0.01, ***p<0.001)

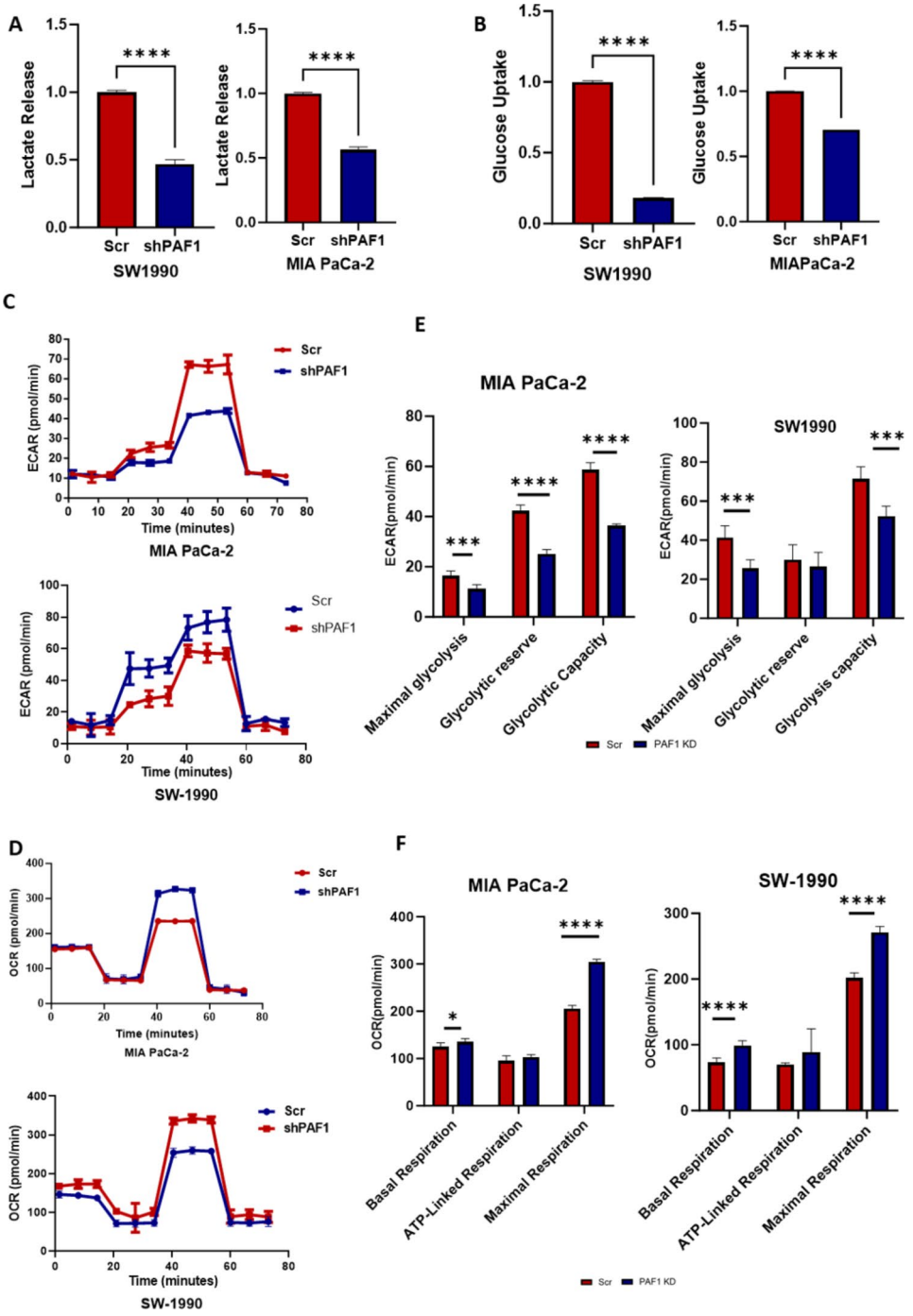

Fig. 3 PAF1 reduction alters metabolism in PDAC. **A** PAF1 depletion reduces extracellular lactate production in SW1990 and MIA-PaCa-2. **B** PAF1 depletion reduces intracellular glucose uptake in SW1990 and MIA PaCa-2 cells. **C** Overall ECAR curve of Scramble and PAF1 KD MIA PaCa-2 and SW1990 cells. Injection order: glucose (10mM), oligomycin (1 μM), and 2-DG (50 mM) for both MIA PaCa-2 and SW1990 cells. The overall ECAR curves were plotted as the mean ECAR ± SD of six replicates. **D** Overall oxygen consumption rate (OCR) curve of Scramble and PAF1 KD MIA PaCa-2 and SW1990 cells. Injection order: oligomycin (1 μM), FCCP (0.5 μM), and rotenone/ antimycin A (0.5 μM) for both MIA PaCa-2 and SW1990 cells. The overall OCR curves were plotted as the mean OCR ± SD of six replicates. **E** Bar graph showing the glycolysis capacity, Maximal Glycolysis and Glycolytic reserve of Scramble and PAF1 KD MIA PaCa-2 and SW1990 cells. **F** Bar graph showing the basal respiration, ATP-linked respiration and maximal respiration of Scramble and PAF1 KD MIA PaCa-2 and SW1990 cells. Data are presented as the mean ± SD (ns, not significant, $^{**}P < 0.01$; $^{***}P < 0.001$; $^{****}P < 0.0001$). The representative images represent the mean ECAR and OCR ± SD of six replicates respectively

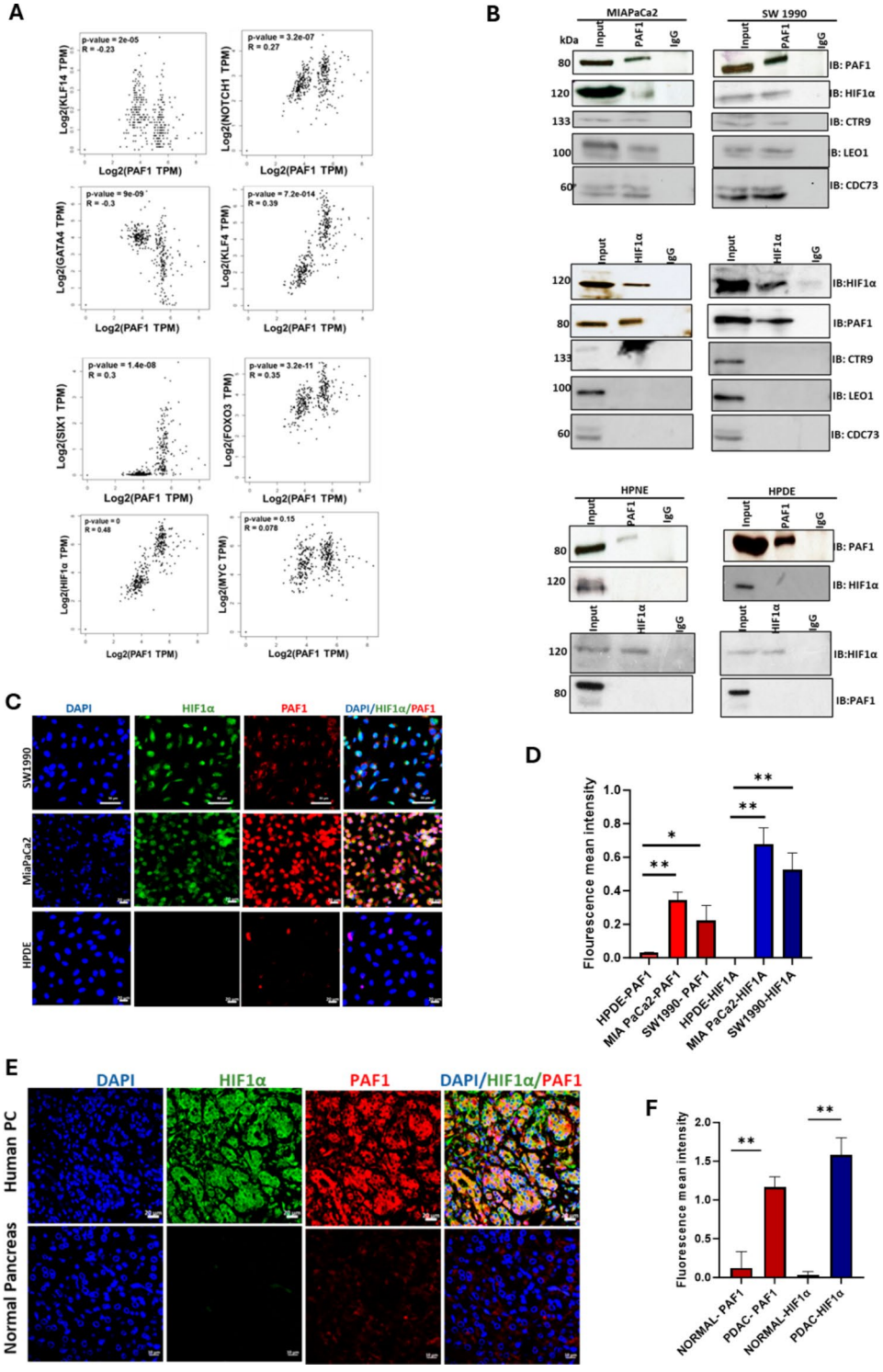

Fig. 4 PAF1 is co-expressed and interacts with HIF1α in PDAC. **A** Multiple correlation analysis between PAF1 and selected aerobic glycolysis transcription factors **B** Immunoprecipitation assay. PAF1 or HIF1α pulldown followed by immunoblotting with HIF1α, PAF1, LEO1, CDC73, CTR9 in indicated samples. Immunofluorescence images of **C.** SW1990, MIA PaCa-2, HPDE cell lines stained with PAF1 and HIF1α antibody. Scale bar 20 μm **D**. Fluorescence mean intensity quantification of HIF1α and PAF1 expression in Fig. 2 (C) **E**. Immunofluorescence images of Human PDAC and normal pancreas tissues stained with PAF1 and HIF1α antibody. Scale bar 20 μm. **F**. Fluorescence mean intensity quantification of HIF1α and PAF1 expression in Fig. 2(E)

transcription factors we identified, only HIF1α significantly correlates with PAF1 (Fig. 4A). We validated this observation by performing an immunoprecipitation assay to ascertain the interaction between PAF1 and HIF1α. The immunoprecipitation of PAF1 or HIF1α was followed by immunoblotting with HIF1α or PAF1 respectively and showed a clear interaction between these two molecules in PDAC (SW1990 and MIA PaCa-2) cells; however, this interaction was not observed in HPDE and HPNE - normal cells (Fig. 4B). These findings suggest that PAF1 interacts with HIF1α specifically in PDAC cells, and not in normal pancreatic cells. Furthermore, we observed an interaction between PAF1 and other subunits of the PAF1 complex, including LEO1, CTR9, and CDC73 in SW1990 and MIA PaCa-2. However, no interaction was observed between HIF1α and other PAF1 complex subunits. Consequently, it is possible that PAF1 forms a sub-complex with HIF1α in PCs, which does not include LEO1, CTR9, and CDC73 (Fig. 4B).

Immunofluorescence staining showed that human PC cell lines (SW1990 and MIA PaCa-2) exhibit high PAF1 and HIF1α expression; however, normal pancreas cells (HPDE) showed basal expression of PAF1($p=0.0062$; $p=0.0152$) and low expression of HIF1α ($p=0.0069$; $p=0.0113$) (Fig. 4C and D). This observation was validated in PDAC tissues as immunofluorescence staining confirmed the co-expression and co-localization of PAF1 ($p=0.0270$) and HIF1α ($p=0.0026$) specifically in PDAC tissues; however, this was totally absent in normal pancreas tissues (Fig. 4E and F). Next, we assessed the impact of PAF1 expression on HIF1α mRNA and protein levels in both normoxia and hypoxia conditions. The qPCR and western blot results indicate that HIF1α mRNA and protein levels in MIA-PaCa-2 PAF1 knockdown cells were not significantly altered in comparison to the Scr cells in both normoxic and hypoxic conditions (Supplementary Fig. 1A, B). In addition, we conducted a colony formation assay under hypoxic conditions. Although the clonogenic growth was significantly reduced as a result of the intensity of the colonies formed, there was no significant difference in the number of colonies formed between the normoxic and hypoxic conditions when PAF1 was knocked down (Supplementary Fig. 2A, B).

Overall, our data shows that PAF1 interacts with HIF1α in PDAC cell lines and is co-expressed with HIF1α in cancer tissues and cells and its co-expression correlates with the progression of the cancer.

PAF1 overexpression increases glycolysis and reduces mitochondrial respiration in PDAC cells

To investigate the impact of PAF1 overexpression on normal cells, we transfected HPDE cells with a plasmid that expressed PAF1. Our findings indicated that PAF1-OE HPDE cells exhibited a substantial increase in the expression of glycolytic genes at both mRNA and protein levels (Fig. 5A, B), compared to vector control. The extracellular acidification rate (ECAR) of HPDE vector and PAF1-OE cells were analyzed using the extracellular flux analyzer to investigate the impact of PAF1 overexpression on the cellular bioenergetics of the normal pancreas cell line. In comparison to vector control cells, HPDE PAF1-OE cells exhibited a substantial increase in the aerobic glycolytic rate (Fig. 5C). Furthermore, various parameters of the aerobic glycolytic rate were analyzed. The results showed that PAF1-overexpression increased glycolytic reserve and glycolytic capacity in HPDE PAF1-OE cells (Fig. 5D). In addition, PAF1 overexpression increased the basal and maximum levels of glycolysis, thus increasing the glucose metabolism in HPDE cells (Fig. 5D).

Additionally, we evaluated oxidative phosphorylation in HPDE vector control and PAF1-OE cells by quantifying the cellular oxygen consumption rate (OCR). PAF1-OE cells exhibited a substantial decrease in OCR compared with the vector control cells (Fig. 5E). Furthermore, mitochondrial respiration indices were evaluated. The data suggested that the maximal respiration of MIA PaCa-2 and SW1990 cells was significantly reduced by PAF1 overexpression (Fig. 5F). Additionally, basal respiration and ATP-linked respiration were substantially diminished (Fig. 5F). In general, the data suggested that the overexpression of PAF1 resulted in an increase in glycolysis and a suppression of mitochondrial respiration in normal cells.

PAF1/HIF1α binds to the LDHA promoter and alters metabolism in PC

Since previous investigations showed that PAF1 interacts with HIF1α and its overexpression in PDAC upregulates LDHA and other critical genes of the aerobic glycolysis pathway, we sought to examine whether the PAF1/HIF1α subcomplex is recruited the LDHA gene promoter. We proceeded to search for HIF1α binding sites on the LDHA promoter using the JASPAR database (Fig. 6A). We found three HIF1α binding sites on the LDHA promoter (Fig. 6B). The chromatin immunoprecipitation (ChIP) assay showed the recruitment of PAF1/HIF1α to the LDHA promoter through the binding site one (B.S.1) (Fig. 6C). The results were subsequently validated through a ChIP-re-ChIP assay-PAF1/HIF1α pull-down. The pull-down was analyzed using PCR, and the result showed that the PAF1/HIF1α subcomplex binds the LDHA promoter through the first binding site (Fig. 6D). However, the PAF1/HIF1α subcomplex binding was absent in MIA PaCa-2 PAF1 knockdown cells (Fig. 6E). These results indicate that PAF1/HIF1α complex binds to the LDHA promoter leading to the transcriptional activation of LDHA in PDAC.

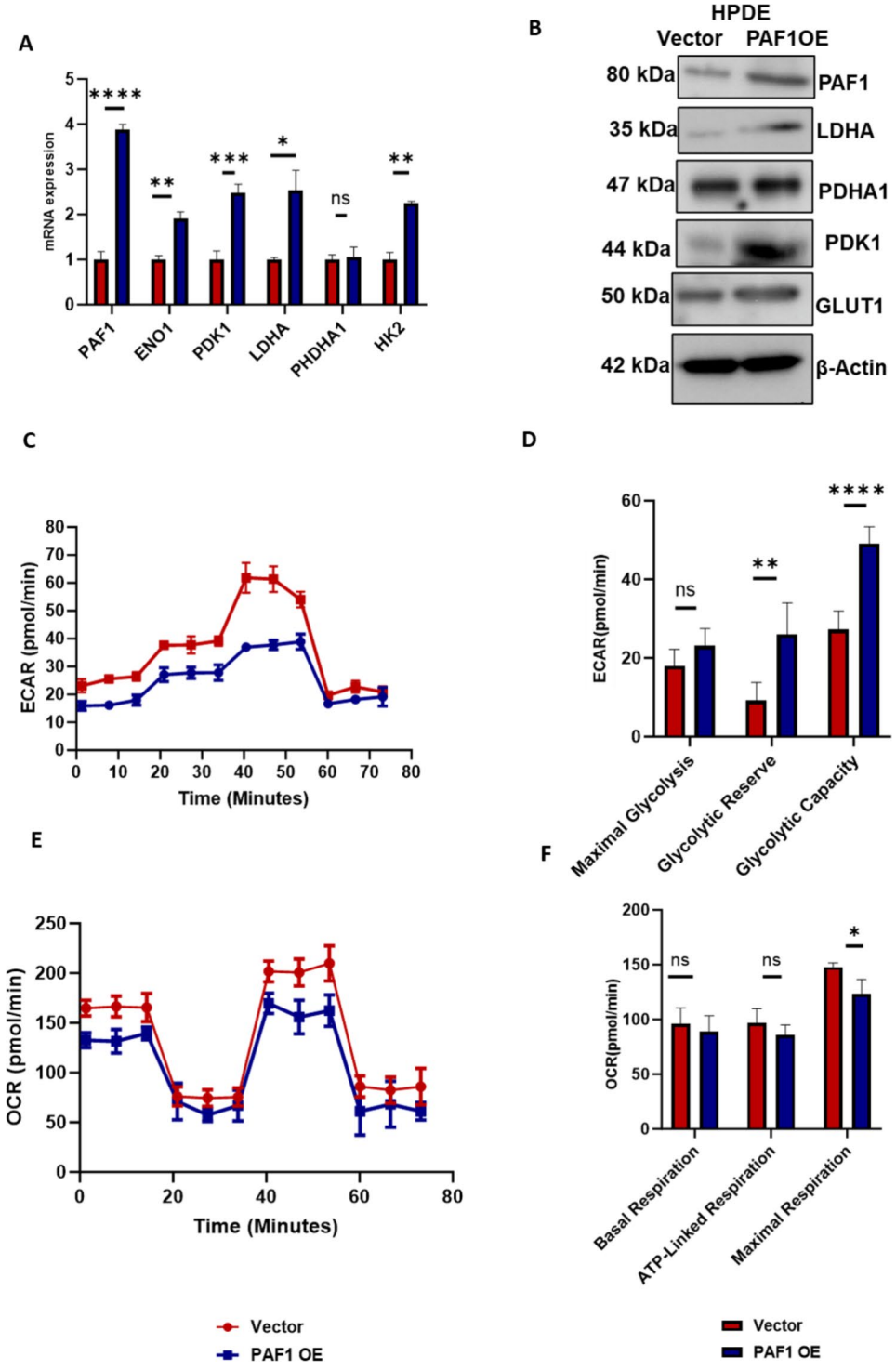

Fig. 5 PAF1 overexpression increases glycolytic rate and reduces mitochondrial respiration in normal cells. **A** qRT-PCR analysis of PAF1, LDHA, PDK1, HK2, PDHA1 and ENO1 in HPDE vector and PAF1 OE cells, qRT-PCR data were normalized with the β-Actin gene. **B** Western blot analysis of PAF1 and aerobic glycolysis genes expression in PAF1 OE and Vector HPDE cells, β-actin was used as a control. **C** Overall ECAR curve of Vector and PAF1OE HPDE cells. Injection order: glucose (10mM), oligomycin (1 μM), and 2-DG (50 mM). The overall ECAR curves were plotted as the mean ECAR ± SD of six replicates. **D** Bar graph showing the glycolysis capacity, Maximal Glycolysis and Glycolytic reserve of Vector and PAF1OE HPDE cells. **E** Overall oxygen consumption rate (OCR) curve of Vector and PAF1OE HPDE cells. Injection order: oligomycin (1 μM), FCCP (0.5 μM), and rotenone/ antimycin A (0.5 μM). The overall OCR curves were plotted as the mean OCR ± SD of six replicates. **F** Bar graph showing the basal respiration, ATP-linked respiration and maximal respiration of Vector and PAF1OE HPDE cells. Data are presented as the mean ± SD (ns, not significant, $^{**}P < 0.01$; $^{***}P < 0.001$; $^{****}P < 0.0001$). The representative images represent the mean ECAR and OCR ± SD of six replicates respectively

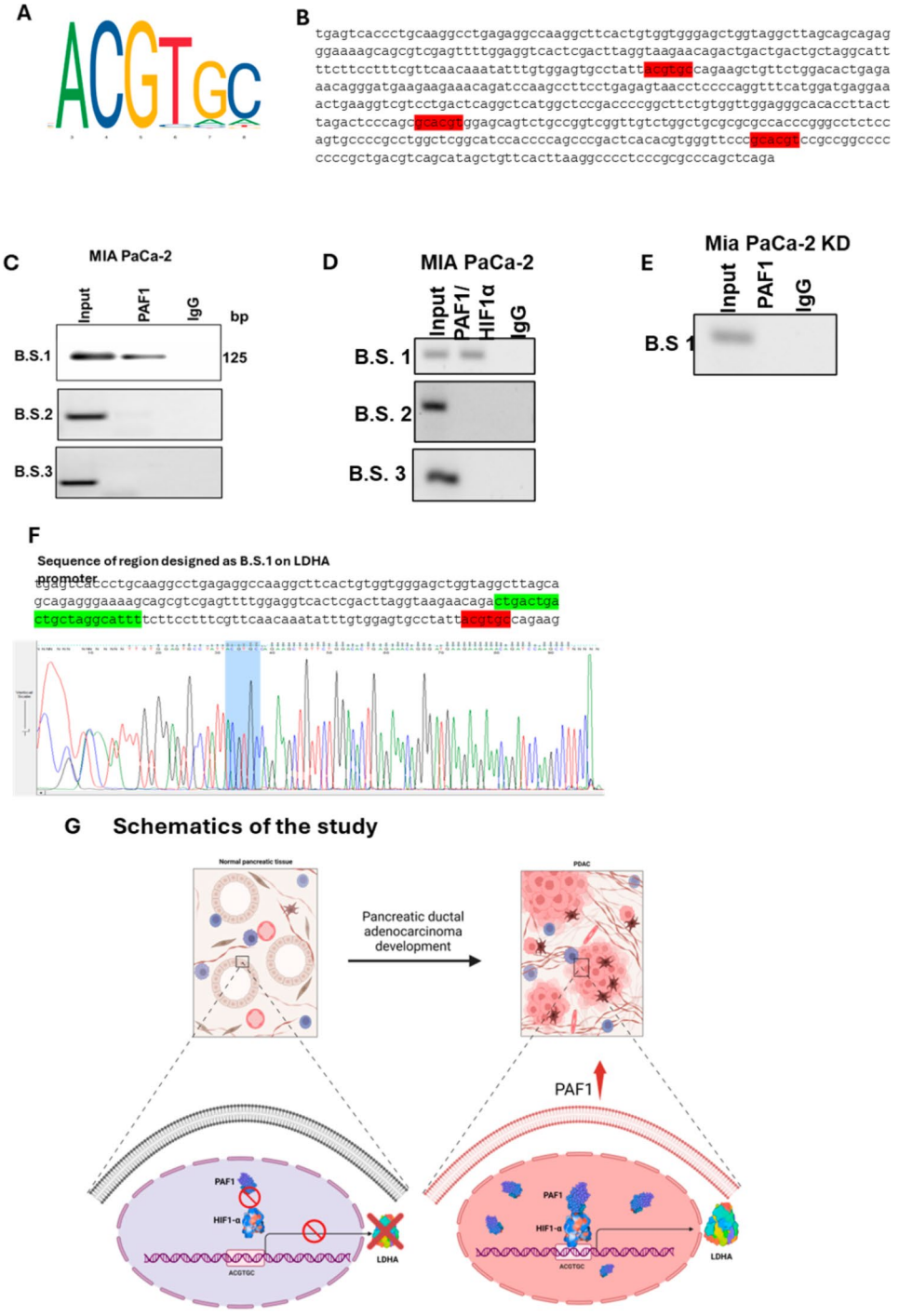

Fig. 6 PAF1 regulates LDHA transcription through HIF1α binding. **A** Consensus Human HIF1α binding motif generated on https://jaspar.genereg.net/. **B** LDHA promoter sequence showing three HIF1α binding sites. **C** ChIP assay was performed using PAF1 and control IgG antibodies in MiaPaCa2 cells using primers that amplify LDHA promoter, which contains HIF1α binding motif. Immunoprecipitated and purified DNA was amplified using PCR followed by running in agarose gel. Binding site 2 and 3 did not amplify. **D** ChIP Re-ChIP assay was performed using PAF1, HIF1α and control IgG antibodies in Mia-PaCa2 cells using primers that amplify LDHA promoter. Immunoprecipitated and purified DNA was amplified using PCR followed by running in agarose gel. Binding sites 2 and 3 did not amplify **E** ChIP assay was performed using PAF1 and control IgG antibodies in MiaPaCa2 shPAF1 cells using primers that amplify LDHA promoter for B.S.1. Immunoprecipitated and purified DNA was amplified using PCR followed by running in agarose gel. Binding site 1 did not amplify. **F** Representative sequence generated from PCR amplification and purification, with HIF1α binding motif highlighted. **G** Schematic shows the overall summary of the study

Discussion

One of the hallmarks of cancer is unconstrained proliferation and their increased need for biomass, macromolecules, and energy. Numerous studies have shown that vital oncogenic drivers and mutations in PDAC play a role in dysregulating cellular metabolism [20, 21]. For instance, KRAS, one of the significant driver mutations leading to PDAC, plays an essential role in the selective maintenance of glucose flux by upregulating the expression of glucose transporter −1(GLUT1). This enhanced glycolytic activity supports the tumor growth [22]. Moreover, KrasG12D-mutated pancreatic cancer cells display elevated glycolytic activity through the nonoxidative branch of the pentose phosphate pathway (PPP) [23]. Also, a previous study showed that p53 is capable of blocking G6PD activity through transient interaction. Suppression of p53 in tumor cells is predicted to increase glucose intake while directing it for biomass synthesis through an increase in the PPP flux [24]. It also means that p53, a tumor suppressor gene and one of the four primary driver mutations in PDAC, might be involved in oxidative PPP in PDAC tumor cells [24]. Another study recently identified SIRT5 as a major tumor suppressor in PDAC, showing that the absence of SIRT5 favors tumorigenesis by increasing noncanonical glutamine metabolism facilitated by GOT1 [25]. Despite the previous research in the field, there is a continuous need to identify novel regulators of metabolic reprogramming, their molecular mechanisms, and the drugs that can inhibit these specific metabolic pathways, which are crucial to improving the overall prognosis of the disease. Beyond the transcriptional role of PAF1 in the context of the PAF1 complex in normal cells [26], we have previously demonstrated that PAF1 contributes to the development and progression of pancreatic cancer through several targets, and often, it does this independently of its complex subunits [27, 28].

Several pancreatic cancer studies have demonstrated the overexpression of LDHA in both cell lines and clinical specimens and identified that the forced expression of LDHA encouraged tumor growth, thereby increasing the tumorigenicity and aggressiveness of pancreatic cancer [4]. Consistent with this, in-silico analysis showed that PAF1 overexpression in pancreatic cancer results in an upregulation of both oxidative phosphorylation and aerobic glycolysis. However, we observed that PAF1 depletion resulted in LDHA downregulation and the downregulation of other critical drivers of aerobic glycolysis. Interestingly, our immunohistochemistry and immunofluorescence data showed differential and increasing expression of PAF1 and LDHA in PDAC tissues. In contrast, there was basal expression of PAF1 and LDHA in normal pancreas. Furthermore, there was co-expression between these two proteins in PC cell lines, further validating the role of PAF1 in glycolysis and PC metabolic rewiring. While previous studies conducted by our lab have demonstrated that PAF1 expression is closely associated with tumor progression through multiple routes [6, 7, 10, 11, 27, 28], thereby indicating poor survival and prognosis in patients with pancreatic cancer [11, 28], this study showed that inhibition of PAF1 inhibits glucose utilization, lactate production, and decreases extracellular acidification rate, all of which are axes regulated solely by LDHA. In contrast, we observed that HPDE cells, with PAF1 overexpression had an upregulation of aerobic glycolysis genes, increased extracellular acidification rate, and reduced oxygen consumption rate, indicating that the initial observation is a direct effect of PAF1.

Forced expression of LDHA promotes increased lactate production, which contributes to the acidification of the tumor microenvironment [29], a microenvironment already plagued with hypoxia, resulting in HIF1α accumulation. Following this, we observed that PAF1 interacts with HIF1α specifically in pancreatic cancer cell lines but not in normal pancreas. Interestingly, while previous studies have shown that PAF1 complex subunits- LEO1, CTR9, and CDC73 interact with PAF1, we observed no interaction between LEO1, CTR9, CDC73, and HIF1α in PCs, reiterating that the PAF1 sub-complex with HIF1α is unique to PCs, and independent of the other PAF1C subunits.

In addition, we investigated the presence of potential binding sites of HIF1α on LDHA binding sites since there has been no evidence of PAF1 directly binding to dsDNA. Consistent with previous studies, we found three HIF1α binding motifs on the LDHA promoter [30]. However, our ChIP results showed the presence of PAF1-HIF1α subcomplex binding to one of the binding motifs of HIF1α. We also observed that PAF1/HIF1α subcomplex binds to the LDHA promoter and activate LDHA transcription, which was absent in PAF1 knockdown cells, thereby regulating LDHA expression in pancreatic cancer.

In conclusion, our study provided both in-vitro and mechanistic evidence supporting that PAF1 modulates LDHA expression. The PAF1/HIF1α axis is critical in metabolic rewiring, aerobic glycolysis, and tumor progression in pancreatic cancer. Our research identified the dysregulated PAF1–LDHA axis as a promising new molecular target for designing novel therapies to control the development and progression of pancreatic cancer.

Supplementary Information

The online version contains supplementary material available at https://doi.org/10.1186/s40170-024-00354-2.

Supplementary Material 1

Supplementary Material 2

Acknowledgements
We thank Kavita Mallya and Bertina Williams for their technical help in the laboratory. We thank Janice Taylor and James R. Talaska of Advanced Microscopy Core Facility, University of Nebraska Medical Center, for their confocal microscopy assistance.

Author contributions
AOO and MPP conceived and designed the experiments. AOO performed the experiments. NG, SR, SM, RKN, and JLC assisted in performing the experiments. AOO, MPP, ZWA and JLC analyzed the data. AOO wrote the manuscript. AOO, MPP, SKB, NG, SM reviewed and edited the manuscript.

Funding
The authors in this article were supported primarily by the following grants from the National Institutes of Health R01CA273349, R01CA263575, R01CA256973, R01CA206444, R01CA210637, R01CA228524, R01CA273319, U01CA200466, U01CA210240, P01CA217798, and Nebraska Stem Cell Grant LB606/2022-10.

Data availability
No datasets were generated or analysed during the current study.

Declarations

Ethical approval
Not applicable.

Competing interests
SKB is one of the co-founders of Sanguine Diagnostics and Therapeutics, Inc. The other authors declare no competing interests.

Received: 9 February 2024 / Accepted: 19 August 2024
Published online: 06 September 2024

References

1. https://seer.cancer.gov/statfacts/html/common.html#:~:text=Pancreatic%20cancer%20is%20the%20third,of%20all%20expected%20cancer%20deaths. [.
2. Karasinska JM, Topham JT, Kalloger SE, Jang GH, Denroche RE, Culibrk L, et al. Altered gene expression along the glycolysis-cholesterol synthesis Axis is Associated with Outcome in Pancreatic Cancer. Clin Cancer Res. 2020;26(1):135–46.
3. Heid I, Münch C, Karakaya S, Lueong SS, Winkelkotte AM, Liffers ST, et al. Functional noninvasive detection of glycolytic pancreatic ductal adenocarcinoma. Cancer Metab. 2022;10(1):24.
4. Rong Y, Wu W, Ni X, Kuang T, Jin D, Wang D, Lou W. Lactate dehydrogenase A is overexpressed in pancreatic cancer and promotes the growth of pancreatic cancer cells. Tumour Biol. 2013;34(3):1523–30.
5. Son J, Lyssiotis CA, Ying H, Wang X, Hua S, Ligorio M, et al. Glutamine supports pancreatic cancer growth through a KRAS-regulated metabolic pathway. Nature. 2013;496(7443):101–5.
6. Moniaux N, Nemos C, Schmied BM, Chauhan SC, Deb S, Morikane K, et al. The human homologue of the RNA polymerase II-associated factor 1 (hPaf1), localized on the 19q13 amplicon, is associated with tumorigenesis. Oncogene. 2006;25(23):3247–57.
7. Vaz AP, Deb S, Rachagani S, Dey P, Muniyan S, Lakshmanan I, et al. Overexpression of PD2 leads to increased tumorigenicity and metastasis in pancreatic ductal adenocarcinoma. Oncotarget. 2016;7(3):3317–31.
8. Karmakar S, Dey P, Vaz AP, Bhaumik SR, Ponnusamy MP, Batra SK. PD2/PAF1 at the crossroads of the Cancer Network. Cancer Res. 2018;78(2):313–9.
9. Dey P, Rachagani S, Vaz AP, Ponnusamy MP, Batra SK. PD2/Paf1 depletion in pancreatic acinar cells promotes acinar-to-ductal metaplasia. Oncotarget. 2014;5(12):4480–91.
10. Karmakar S, Seshacharyulu P, Lakshmanan I, Vaz AP, Chugh S, Sheinin YM, et al. hPaf1/PD2 interacts with OCT3/4 to promote self-renewal of ovarian cancer stem cells. Oncotarget. 2017;8(9):14806–20.
11. Karmakar S, Rauth S, Nallasamy P, Perumal N, Nimmakayala RK, Leon F, et al. RNA polymerase II-Associated factor 1 regulates stem cell features of pancreatic Cancer cells, independently of the PAF1 complex, via interactions with PHF5A and DDX3. Gastroenterology. 2020;159(5):1898–e9156.
12. Zhi X, Giroux-Leprieur E, Wislez M, Hu M, Zhang Y, Shi H, et al. Human RNA polymerase II associated factor 1 complex promotes tumorigenesis by activating c-MYC transcription in non-small cell lung cancer. Biochem Biophys Res Commun. 2015;465(4):685–90.
13. Zheng J-J, He Y, Liu Y, Li F-S, Cui Z, Du X-M, et al. Novel role of PAF1 in attenuating radiosensitivity in cervical cancer by inhibiting IER5 transcription. Radiat Oncol. 2020;15(1):131.
14. Massett ME, Monaghan L, Patterson S, Mannion N, Bunschoten RP, Hoose A, et al. A KDM4A-PAF1-mediated epigenomic network is essential for acute myeloid leukemia cell self-renewal and survival. Cell Death Dis. 2021;12(6):573.
15. Qin C, Yang G, Yang J, Ren B, Wang H, Chen G, et al. Metabolism of pancreatic cancer: paving the way to better anticancer strategies. Mol Cancer. 2020;19(1):50.
16. Rashid M, Zadeh LR, Baradaran B, Molavi O, Ghesmati Z, Sabzichi M, Ramezani F. Up-down regulation of HIF-1α in cancer progression. Gene. 2021;798:145796.
17. Tao J, Yang G, Zhou W, Qiu J, Chen G, Luo W, et al. Targeting hypoxic tumor microenvironment in pancreatic cancer. J Hematol Oncol. 2021;14(1):14.
18. Hu Q, Qin Y, Ji S, Xu W, Liu W, Sun Q, et al. UHRF1 promotes aerobic glycolysis and proliferation via suppression of SIRT4 in pancreatic cancer. Cancer Lett. 2019;452:226–36.
19. Erkan M, Hausmann S, Michalski CW, Fingerle AA, Dobritz M, Kleeff J, Friess H. The role of stroma in pancreatic cancer: diagnostic and therapeutic implications. Nat Rev Gastroenterol Hepatol. 2012;9(8):454–67.
20. Pavlova NN, Thompson CB. The emerging Hallmarks of Cancer Metabolism. Cell Metab. 2016;23(1):27–47.
21. Ogunleye AO, Nimmakayala RK, Batra SK, Ponnusamy MP. Metabolic rewiring and stemness: a critical attribute of pancreatic Cancer progression. Stem Cells. 2023;41(5):417–30.
22. Gaglio D, Metallo CM, Gameiro PA, Hiller K, Danna LS, Balestrieri C, et al. Oncogenic K-Ras decouples glucose and glutamine metabolism to support cancer cell growth. Mol Syst Biol. 2011;7:523.
23. Ying H, Kimmelman AC, Lyssiotis CA, Hua S, Chu GC, Fletcher-Sananikone E, et al. Oncogenic Kras maintains pancreatic tumors through regulation of anabolic glucose metabolism. Cell. 2012;149(3):656–70.
24. Jiang P, Du W, Wang X, Mancuso A, Gao X, Wu M, Yang X. p53 regulates biosynthesis through direct inactivation of glucose-6-phosphate dehydrogenase. Nat Cell Biol. 2011;13(3):310–6.
25. Hu T, Shukla SK, Vernucci E, He C, Wang D, King RJ, et al. Metabolic rewiring by loss of Sirt5 promotes Kras-Induced Pancreatic Cancer Progression. Gastroenterology. 2021;161(5):1584–600.
26. Fischl H, Howe FS, Furger A, Mellor J. Paf1 has distinct roles in transcription elongation and Differential transcript fate. Mol Cell. 2017;65(4):685–e988.
27. Nimmakayala RK, Ogunleye AO, Parte S, Krishna Kumar N, Raut P, Varadharaj V, et al. PAF1 cooperates with YAP1 in metaplastic ducts to promote pancreatic cancer. Cell Death Dis. 2022;13(10):839.
28. Rauth S, Ganguly K, Atri P, Parte S, Nimmakayala RK, Varadharaj V, et al. Elevated PAF1-RAD52 axis confers chemoresistance to human cancers. Cell Rep. 2023;42(2):112043.
29. Porporato PE, Dhup S, Dadhich RK, Copetti T, Sonveaux P. Anticancer targets in the glycolytic metabolism of tumors: a comprehensive review. Front Pharmacol. 2011;2:49.
30. Zheng F, Chen J, Zhang X, Wang Z, Chen J, Lin X, et al. The HIF-1α antisense long non-coding RNA drives a positive feedback loop of HIF-1α mediated transactivation and glycolysis. Nat Commun. 2021;12(1):1341.

Publisher's note